Pergamon

*Int. J. Heat Mass Transfer.* Vol. 38, No. 3, pp. 481–493, 1995

0017-9310/95 $9.50+0.00

0017-9310(94)00183-9

# Foundation of the interfacial area transport equation and its closure relations

G. KOCAMUSTAFAOGULLARI

Department of Mechanical Engineering, University of Wisconsin–Milwaukee, Milwaukee, WI 53201, U.S.A.

and

M. ISHII

School of Nuclear Engineering, Purdue University, West Lafayette, IN 47907, U.S.A.

(*Received* 1 *October* 1993 *and in final form* 2 *June* 1994)

**Abstract**—The interfacial area transport equation is derived from the statistical model of fluid particle number transport equation. The resulting equation includes the source and sink terms due to the particle interactions and interfacial phase change. The consistency of this new approach is demonstrated in terms of the macroscopic continuity equation of a bubbly flow field. The basic mechanisms affecting these source and sink terms are discussed. The general framework to develop the closure relations for the fluid particle interaction and phase change terms is presented. Finally, the one-dimensional interfacial area transport equation is used to identify possible methods to relate the source and sink terms to experimentally measurable interfacial parameters, such that experiments can be used to establish models for these terms.

## 1. INTRODUCTION

The interfacial transfer terms are strongly related to the interfacial area and to the local mechanisms, such as the degree of turbulence near the interfaces. Basically, the interfacial transport of mass, momentum and energy is proportional to the interfacial area concentration and to a driving force. This area concentration, defined as the interfacial area per unit volume of the mixture, characterizes the kinematic effects; therefore, it must be related to the structure of the two-phase flow field. On the other hand, the driving forces for the interphase transport characterize the local transport mechanism, and they must be modeled separately.

Basic macroscopic parameters related to the internal structure of two-phase flows, particularly of a dispersed (bubbly or droplet) flow, are the void fraction, particle number density, interfacial area concentration and the particle shape factor. From geometric considerations, it is demonstrated by Kocamustafaogullari and Ishii [1] and Kocamustafaogullari *et al.* [2] that the particle number density is a key parameter in determining the interfacial area concentration, but it has not been sufficiently investigated in the literature.

Realizing the significance of the fluid particle number density as an important parameter for predicting the interfacial area concentration in a forced convective two-phase flow channel, the following are the objectives of this work:

1. to formulate the fluid particle number density transport in terms of the differential balance equation which takes into account various parameters such as the fluid particle generation and disintegration rates through the source and/or sink terms;
2. to develop the fluid particle interfacial area concentration transport equation,
3. to discuss the physical significance and possible mechanisms for particle interaction terms that give rise to the rate of change of number density due to sources and sinks; and
4. to demonstrate a possible method to relate these source and sink terms to experimentally measured interfacial parameters, such that experiments can be used to establish a model for these terms.

## 2. FLUID PARTICLE TRANSPORT EQUATIONS

### 2.1. *Fluid particle number density transport equation*

For the analysis of dispersive systems in agitated vessels, the fluid particle number density transport equation has been extensively and successfully used over the past three decades [3–6]. The fluid particle interfacial transport equations for the interfacial area concentration and void fraction can be developed from the fluid particle number density transport equation analogous to Boltzmann's transport equation. This approach recently was proposed by Reyes [7] to develop a set of fluid particle conservation equations for a distribution of chemically non-reacting, spherical fluid particles dispersed in a continuous medium. Here

## NOMENCLATURE

| | |
|---|---|
| $A$ | cross-sectional area |
| $A_i$ | interfacial area of a particle |
| $a_i$ | interfacial area concentration |
| $D$ | hydraulic diameter of flow channel |
| $d$ | fluid particle diameter |
| $d_{dp}$ | bubble departure diameter |
| $f$ | particle density distribution function |
| $f_{dp}$ | bubble departure frequency |
| $g$ | break-up frequency of particles |
| $h$ | collision frequency |
| $i$ | specific enthalpy |
| $i_{fg}$ | heat of evaporation |
| $N$ | total number of particles per unit volume of mixture |
| $Na$ | nucleation site density |
| $n$ | number of daughter particles produced by break-up |
| $Re_c$ | continuous phase particle Reynolds number |
| $Re_d$ | dispersed phase particle Reynolds number |
| $r$ | radial coordinate |
| $r_d$ | fluid particle radius |
| $S_{ph}$ | formation or loss rate of particles per unit volume of mixture due to phase change |
| $S_1$ | formation rate of particles per unit volume of mixture due to break-up |
| $S_2$ | loss rate of particles per unit volume of mixture due to break-up |
| $S_3$ | formation rate of particles per unit volume of mixture due to coalescence |
| $S_4$ | loss rate of particles per unit volume of mixture due to coalescence |
| $T$ | temperature |
| $t$ | time |
| $v$ | volume of a particle |
| $\vec{v}$ | velocity vector |
| $\vec{v}_g$ | gaseous phase center of mass velocity |
| $\vec{v}_i$ | interfacial velocity |
| $\vec{v}_p$ | particle velocity |
| $\vec{v}_{pm}$ | average particle velocity weighted by particle number |
| $\vec{v}_r$ | relative velocity |
| $\vec{x}$ | position vector |
| $We_{cr}$ | critical Weber number |
| $z$ | axial flow direction. |

Greek symbols

| | |
|---|---|
| $\alpha$ | void fraction |
| $\beta$ | distribution of daughter particles upon break-up |
| $\Gamma_g$ | rate of interfacial phase change per unit volume of mixture |
| $\varepsilon$ | energy dissipation rate per unit mass |
| $\lambda$ | coalescence efficiency |
| $\mu$ | dynamic viscosity |
| $\nu$ | kinematic viscosity |
| $\xi_h$ | heated perimeter |
| $\rho$ | density |
| $\tau$ | external stresses |
| $\phi_{ph}$ | rate of change of interfacial area concentration due to phase change |
| $\phi_1$ | rate of change of interfacial area concentration due to break-up |
| $\phi_2$ | rate of change of interfacial area concentration due to break-up |
| $\phi_3$ | rate of change of interfacial area concentration due to coalescence |
| $\phi_4$ | rate of change of interfacial area concentration due to coalescence. |

Subscripts

| | |
|---|---|
| c | continuous phase |
| d | dispersed phase |
| f | liquid phase |
| g | gaseous phase |
| w | wall |
| sat | saturation condition. |

we shall follow a similar approach and extend the model for a general two-phase flow.

A simple procedure accounting for the fluid particle entering and leaving a control volume through different mechanisms yields the fluid particle number density transport equation of particles having volume $v$:

$$\frac{\partial f}{\partial t}+\nabla\cdot(f\vec{v}_p)=\sum_{j=1}^{4}S_j+S_{ph}. \tag{1}$$

In this equation, $f(\vec{x}, v, t)$ is the particle density distribution function, which is assumed to be continuous and specifies the probable number density of fluid particles at a given time $t$, in the spatial range $d\vec{x}$ about a position $\vec{x}$, with particle volumes between $v$ and $v+dv$. $\vec{v}_p(\vec{x}, v, t)$ is the particle velocity of volumes between $v$ and $v+dv$ at time $t$. $S_{ph}$ is the fluid particle sink or source rate due to the phase change. For example, for one component bubbly flow $S_{ph}$ represents the bulk liquid bubble nucleation rate due to the homogeneous and heterogeneous nucleation, and the collapse rate due to condensation for the subcooled boiling flow. The significance and methods evaluating $S_{ph}$ are discussed in great detail by Kocamustafaogullari and Ishii [1]. The wall nucleation rate which is not included in $S_{ph}$ must be specified as a boundary condition.

The interaction term, $\sum_{j=1}^{4}S_j$, represents the net rate of change in the number density distribution func-

tion, $f$, due to the particle break-up and coalescence processes. In essence, it serves as source and/or sink terms for fluid particles for two-component dispersed two-phase flow. $S_1$ and $S_2$, respectively, represent the formation and loss rates of particles of volume $v$ per unit volume of mixture due to break-up. $S_3$ and $S_4$ represent the rate of formation and loss of particles of size $v$ due to coalescence. These terms are given in the following equations:

$$S_1(\vec{x}, v, t) = \int_v^{v_{max}} \beta(v', v) n(v') g(v') f(\vec{x}, v', t)\, dv' \tag{2}$$

$$S_2(\vec{x}, v, t) = -g(v) f(\vec{x}, v, t) \tag{3}$$

$$S_3(\vec{x}, v, t) = \int_{v_{min}}^{v/2} \lambda(v-v', v') h(v-v', v') \times f(\vec{x}, v-v', t) f(\vec{x}, v', t)\, dv' \tag{4}$$

$$S_4(\vec{x}, v, t) = -\int_{v_{min}}^{v_{max}-v} \lambda(v, v') h(v, v') \times f(\vec{x}, v', t) f(\vec{x}, v, t)\, dv'. \tag{5}$$

Here, $g(v')$ is the break-up frequency of a particle having a volume of $v'$; $\beta(v', v)$ is the distribution of daughter particles produced upon break-up of a parent particle having volume $v'$; $n(v')$ is the number of daughter particles produced by break-up of a parent particle of $v'$; $\lambda(v, v')$ is the coalescence efficiency once collision occurs between particles of volume $v$ and $v'$; $h(v, v')$ is the collision frequency of particles of volumes $v$ and $v'$; and $v_{min}$ and $v_{max}$, respectively, are the minimum and maximum particle volumes.

The fluid particle number density transport equation of particles having volume of $v$ described by equation (1) is much too detailed for most flow studies where the primary focus is on the average fluid particle behavior. Therefore, it would be advantageous to develop a particle number density transport equation that has been averaged over all particle sizes. It can be achieved by integration of equation (1) from the minimum particle volume to the maximum possible particle volume. Thus,

$$\int_{v_{min}}^{v_{max}} \frac{\partial f}{\partial t} dv + \int_{v_{min}}^{v_{max}} \nabla \cdot f \vec{v}_p\, dv = \sum_{j=1}^{4} \int_{v_{min}}^{v_{max}} S_j\, dv + \int_{v_{min}}^{v_{max}} S_{ph}\, dv. \tag{6}$$

Applying the Leibnitz rule for integration and noting that:

$$\int_{v_{min}}^{v_{max}} f(\vec{x}, v, t)\, dv = N(\vec{x}, t) \tag{7}$$

the number density transport equation can be expressed as follows:

$$\frac{\partial N}{\partial t} + \nabla \cdot N \vec{v}_{pm} = \sum_{j=1}^{4} \int_{v_{min}}^{v_{max}} S_j\, dv + \int_{v_{min}}^{v_{max}} S_{ph}\, dv \tag{8}$$

where $N(\vec{x}, t)$ is the total number of particles of all sizes per unit volume of mixture, and $\vec{v}_{pm}(\vec{x}, t)$ is the average local particle velocity weighted by the particle number. It is defined by:

$$\vec{v}_{pm}(\vec{x}, t) \equiv \frac{\int_{v_{min}}^{v_{max}} f(\vec{x}, v, t) \vec{v}_p(\vec{x}, v, t)\, dv}{\int_{v_{min}}^{v_{max}} f(\vec{x}, v, t)\, dv}. \tag{9}$$

Equation (1) will serve as the basis for the development of the interfacial area concentration and void fraction transport equations.

### 2.2. *Fluid particle interfacial area concentration transport equation*

The interfacial area concentration transport equation of particles of volume $v$ can be obtained by multiplying the particle number density transport equation of particles having volume $v$ by the average interfacial area, $A_i(v)$, of particles of volume $v$, which is independent of the spatial coordinate system. This yields the following equation:

$$\frac{\partial f A_i(v)}{\partial t} + \nabla \cdot (f A_i(v) \vec{v}_p) = \sum_{j=1}^{4} A_i(v) S_j + A_i(v) S_{ph}. \tag{10}$$

As in the case of the fluid particle number density equation, the fluid particle interfacial area concentration transport equation of volume $v$ given by equation (10) is much too detailed for practical purposes. It would be much more useful to develop an interfacial area transport equation averaged over all particle sizes. This can easily be done by integrating equation (10) from $v_{min}$ to $v_{max}$. Thus,

$$\int_{v_{min}}^{v_{max}} \frac{\partial f A_i(v)}{\partial t} dv + \int_{v_{min}}^{v_{max}} \nabla \cdot (f A_i(v) \vec{v}_p)\, dv = \sum_{j=1}^{4} \int_{v_{min}}^{v_{max}} A_i(v) S_j\, dv + \int_{v_{min}}^{v_{max}} A_i(v) S_{ph}\, dv. \tag{11}$$

Again applying the Leibnitz rule, the average interfacial area concentration transport equation can be expressed in a condensed form as follows:

$$\frac{\partial a_i}{\partial t} + \nabla \cdot a_i \vec{v}_i = \sum_{j=1}^{4} \phi_j + \phi_{ph} \tag{12}$$

where $a_i(\vec{x}, t)$ is the average interfacial area concentration of all fluid particles of volumes between $v_{min}$ and $v_{max}$, and $\vec{v}_i(\vec{x}, t)$ is the interfacial velocity. These variables are defined as:

$$a_i(\vec{x}, t) \equiv \int_{v_{min}}^{v_{max}} f(\vec{x}, v, t)\, A_i(v)\, dv \tag{13}$$

and:

$$\vec{v}_i(\vec{x}, t) \equiv \frac{\int_{v_{min}}^{v_{max}} f(\vec{x}, v, t)\, A_i(v)\, \vec{v}_p(\vec{x}, v, t)\, dv}{\int_{v_{min}}^{v_{max}} f(\vec{x}, v, t)\, A_i(v)\, dv}. \tag{14}$$

$\phi_j$s, which are defined by:

$$\phi_j \equiv \int_{v_{min}}^{v_{max}} A_i(v)\, S_j(\vec{x}, v, t)\, dv \quad j = 1, 2, 3, 4 \tag{15}$$

represent the rate of change in the interfacial area concentration due to the particle break-up and coalescence processes. In line with definitions $S_1$, $S_2$, $S_3$ and $S_4$ expressed, respectively, by equations (2)–(5), the following describes each $\phi_j$:

$$\phi_1 = \int_{v_{min}}^{v_{max}} A_i(v) \int_{v}^{v_{max}} \beta(v', v)\, n(v') \times g(v') f(\vec{x}, v', t)\, dv'\, dv \tag{16}$$

$$\phi_2 = -\int_{v_{min}}^{v_{max}} A_i(v)\, g(v) f(\vec{x}, v, t)\, dv \tag{17}$$

$$\phi_3 = \int_{v_{min}}^{v_{max}} A_i(v) \int_{v_{min}}^{v/2} \lambda(v - v', v')\, h(v - v', v') \times f(\vec{x}, v - v', t) f(\vec{x}, v', t)\, dv'\, dv \tag{18}$$

$$\phi_4 = -\int_{v_{min}}^{v_{max}} A_i(v) \int_{v_{min}}^{v_{max}} \lambda(v, v')\, h(v, v') \times f(\vec{x}, v', t) f(\vec{x}, v, t)\, dv'\, dv. \tag{19}$$

From the above equations, it is evident that $\phi_1$ and $\phi_2$, respectively, represent the rate of increase and decrease in the interfacial area concentration due to the fluid particle break-up process, whereas $\phi_3$ and $\phi_4$ describe the rate of increase and decrease due to the coalescence process.

Similarly, $\phi_{ph}$, which is defined by:

$$\phi_{ph} \equiv \int_{v_{min}}^{v_{max}} A_i(v) S_{ph}\, dv \tag{20}$$

represents the rate of interfacial area concentration change due to evaporation or condensation.

### 2.3. *Fluid particle volume fraction (void fraction) transport equation*

The void fraction transport equation of particles having volume $v$ can be obtained by multiplying the particle number density transport equation of particles having volume $v$ by the average volume of particles. This yields the following equation:

$$\frac{\partial f v}{\partial t} + \nabla \cdot (f v \vec{v}_p) = \sum_{i=1}^{4} v S_j + v S_{ph}. \tag{21}$$

As in the case of obtaining the interfacial area concentration transport equation, equation (21) can be integrated to obtain the void fraction transport equation as follows:

$$\int_{v_{min}}^{v_{max}} \frac{\partial f v}{\partial t}\, dv + \int_{v_{min}}^{v_{max}} \nabla \cdot (f v \vec{v}_p)\, dv = \sum_{j=1}^{4} \int_{v_{min}}^{v_{max}} v S_j\, dv + \int_{v_{min}}^{v_{max}} v S_{ph}\, dv. \tag{22}$$

Noting that:

$$\alpha(\vec{x}, t) \equiv \int_{v_{min}}^{v_{max}} f(\vec{x}, v, t) \cdot v\, dv \tag{23}$$

and using equation (7), it can be shown that:

$$\frac{\partial \alpha}{\partial t} + \nabla \cdot \alpha \vec{v} = \int_{v_{min}}^{v_{max}} \left( \sum_{j=1}^{4} v S_j + S_{ph} v \right) dv \tag{24}$$

where $\vec{v}(\vec{x}, t)$ is the average velocity of the center of volume of the dispersed phase. It is defined by:

$$\vec{v}(\vec{x}, t) \equiv \frac{\int_{v_{min}}^{v_{max}} f(\vec{x}, v, t)\, v\, \vec{v}_p(\vec{x}, v, t)\, dv}{\int_{v_{min}}^{v_{max}} f(\vec{x}, v, t)\, v\, dv}. \tag{25}$$

Equation (24) is the fluid particle volume fraction transport equation which represents the volume balance for particles of constant density. Both the interfacial area concentration and void fraction transport equations are the moments of the number density transport equation. Since the weighting functions in these equations are the interfacial area and volume, respectively, the resulting equations yield macroscopic transport of the respective quantities.

The consistency of the above derivations can be justified by considering the gaseous phase continuity equation which is given by:

$$\frac{\partial \alpha \rho_g}{\partial t} + \nabla \cdot \alpha \rho_g \vec{v}_g = \Gamma_g \tag{26}$$

where $\Gamma_g$ is the amount of phase change per unit volume of the mixture, and $\vec{v}_g(\vec{x}, t)$ is the velocity of center of mass of gas phase.

For an incompressible flow with no phase change, equation (26) reduces to:

$$\frac{\partial \alpha}{\partial t} + \nabla \cdot \alpha \vec{v}_g = 0. \tag{27}$$

In this case, the velocity of center of mass, $\vec{v}_g$, reduces to the velocity of center of volume $\vec{v}$ as follows:

$$\vec{v}_g(\vec{x}, t) \equiv \frac{\int_{v_{min}}^{v_{max}} f v \vec{v}_p \rho_g\, dv}{\int_{v_{min}}^{v_{max}} f v \rho_g\, dv} = \vec{v}(\vec{x}, t). \tag{28}$$

Finally, comparing equation (27) with equation (24), it can be noted that:

$$\int_{v_{min}}^{v_{max}} \sum_{j=1}^{4} S_j v \, dv = 0 \tag{29}$$

which indicates that the net volume change due to coalescence and break-up would be zero. This identity can be used for the purpose of measuring $S_j$s for a two-phase flow.

### 2.4. *Closure relation requirements*

The parameters involved in the break-up components of the $S_j$s and $\phi_j$s terms are the maximum fluid particle volume, the average daughter particle distribution function, the average number of daughter particles produced by break-up of a parent fluid particle, and the average break-up frequency. On the other hand, the parameters involved in the coalescence component are the minimum fluid particle volume, the average collision frequency, and the average coalescence efficiency. These parameters which are needed to evaluate the fluid particle number density and the interfacial area concentration distributions are summarized as follows:

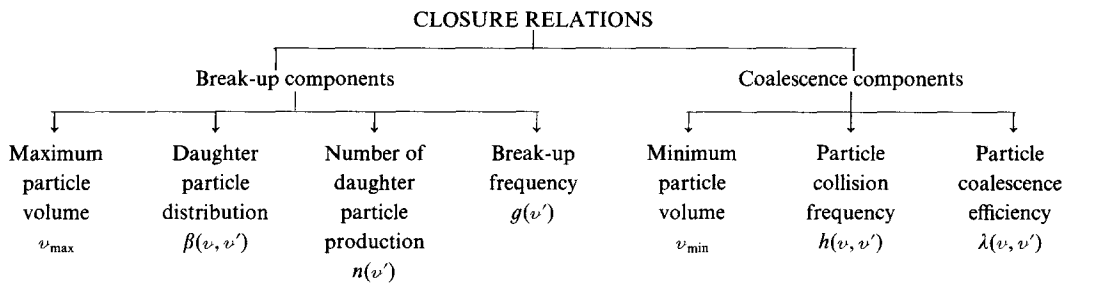


In order to evaluate these terms which serve as source and sink terms in equations (8) and (12), accurate interaction rate models for fluid particle break-up and coalescence must be incorporated. These models are typically functions of the physical and operating conditions of the system. The overall behavior of the particle number density and interfacial area concentration in a region of space can then be predicted by solving the proper transport equation which has the form of an integro-differential equation.

## 3. BREAK-UP AND COALESCENCE MECHANISMS

### 3.1. *Break-up and coalescence processes*

In any two-phase flow field, the initial bubble or drop size is determined in terms of the mechanism of fluid particle generation such as formation of bubbles at an orifice or bubble entrainment mechanisms and generation of droplets by shearing off of roll waves in separated two-phase flow patterns such as annular and stratified-wavy flows. However, in forced convective pipe flow or mechanically agitated systems, the initial fluid particle size may be too large or too small to be stable. In these cases the fluid particle size is further determined by a break-up and/or coalescence mechanism. In boiling systems, in addition to the break-up and coalescence mechanisms, the growth rate should also be considered.

When a fluid particle exceeds a critical value, the particle interface becomes unstable and break-up is likely to occur. Similarly, when fluid particles are smaller than some critical dimension, the coalescence is likely to occur on a series of collision events. Therefore, the particle break-up can be related to the maximum attainable size of the particle; whereas particle coalescence can be related to the minimum size. The literature contains several models for determining the maximum and minimum sizes of fluid particles. These models have been developed from first principles and have been used to develop break-up and coalescence criteria. These criteria, however, do not treat a distribution of fluid particles. Rather, they describe the particle size limits of break-up and coalescence.

In what follows, we shall briefly describe the basic mechanisms that have been used to obtain the closure relations listed in Section 2.4.

### 3.2. *Break-up parameters*

3.2.1. *Maximum fluid particle size*: $d_{max}$ *or* $v_{max}$. The fluid particle break-up controls the maximum bubble or droplet size and can be greatly influenced by the continuous phase hydrodynamics and interfacial interactions. Therefore, a generalized break-up mechanism can be expressed as a balance between external stresses, $\tau$, that attempt to disrupt the bubble and the surface stress, $\sigma/d$, that resists the particle deformation. These stresses influence both the size of fluid particles, which are torn away from their point of formation, and also the maximum particle size which is stable in the flow field. At the point of break-up, these forces must balance. Thus,

$$\tau \propto \sigma/(d/2). \tag{30}$$

This balance leads to the prediction of a critical Weber number, above which the fluid particle is no longer stable. It is defined by:

$$We_{cr} \equiv \tau d_{max}/2\sigma \geqslant 1.0 \tag{31}$$

where $d_{max}$ is the maximum stable fluid particle, and $\tau$ reflects the hydrodynamic conditions responsible for particle deformation and eventual break-up. The mechanism of particle break-up can thus be related to the external conditions as illustrated below:

FLUID PARTICLE BREAK-UP

| Turbulent flow (local turbulence) | Laminar flow (viscous shear) | Interfacial instability (Rayleigh–Taylor and Kelvin–Helmholtz instabilities) |
|---|---|---|

In the case of turbulent flow, particle break-up is caused by fluctuating eddies resulting in the pressure variation along the particle surface. In laminar flow, viscous shear in the continuous phase will elongate the particle and cause break-up. However, even in the absence of net flow of continuous phase such as rising bubbles in a liquid and rising and falling drops in a continuous gas or immiscible liquid, the fluid particle break-up is caused by interfacial instabilities due to the Raleigh–Taylor and Kelvin–Helmholtz instabilities.

Aside from the break-up mechanism caused by interfacial instabilities, basically there are two external forces that are involved in the breaking-up of fluid particles, namely viscous and turbulence induced inertial forces. In most applications, the Reynolds numbers that are characteristic of the flow field are so large that viscous effects are negligible. In other cases, however, inertial effects play a minor role and may be neglected. Existing experimental and theoretical information can, therefore, be classified into two categories, namely, in which surface tension and viscous forces interact, and another in which surface forces and turbulence induced dynamic pressure forces are dominant.

The first fundamental experiments on the break-up of drops and bubbles under the action of external viscous stresses and surface stress were made by Taylor [8]. Taylor made numerous observations, many of which were subsequently explained by Tomotika [9]. The break-up criteria is expressed in terms of external viscous stress in equation (31). It is given by:

$$We_{cr} \equiv \mu_c(\partial v/\partial r)_{max} d_{max}/2\sigma \tag{32}$$

where $\mu_c$ is the absolute viscosity of the continuous phase, and $(\partial v/\partial r)_{max}$ is the maximum velocity gradient in the external flow field. Equation (32) leads to capillary number criteria for break-up.

The Taylor mechanism of bubble and drop deformation applies if both the undeformed and the elongated particles are small compared with the local regions of viscous flow. Several predictive equations for the maximum particle size were derived from equation (32) for agitated vessels [10, 11].

The fluid particle fragmentation phenomenon in a highly turbulent flow is related to the fact that the velocity in a turbulent stream varies from one point to another. The velocity of the fluid particle at the surface of the particle varies from point to point. The velocity of the continuous phase at the surface of the particle also varies from point to point. Therefore, different dynamic pressures will be exerted at different points on the surface of the fluid particle. Under certain conditions, this will inevitably lead to deformation and break-up of the fluid particle.

The force due to dynamic pressure may develop either through the local relative velocity around the particle, which appears because of inertial effects, or through the changes in eddy velocities over the length of the droplet. For both cases, however, the external stress appearing in equation (31) can be expressed in terms of the kinetic energy differences around the droplet. From equation (31), the former yields

$$We_{cr)1} = \rho_c v_{r)max}^2 d_{max}/2\sigma \geqslant 1.0 \tag{33}$$

whereas the latter gives

$$We_{cr)2} = \rho_c \overline{v_c'^2}\, d_{max}/2\sigma \geqslant 1.0. \tag{34}$$

The mean-square spatial fluctuating velocity term, $\overline{v_c'^2}$, describes the turbulent pressure forces of eddies of size $d_{max}$ and is defined as the average of the square of the differences in velocity over a distance equal to the fluid particle diameter. $v_{r)max}$ is that limiting local relative velocity at which a fluid will flow around a particle suspended in it. The subscript c identifies the continuous phase.

Considering the simplest case of turbulence, namely, an isotropic homogeneous turbulence, the main contribution to the kinetic energy, $\overline{v_c'^2}$, is made by the fluctuations in the region of wavelengths where the Kolmogoroff energy distribution is valid. In this region, the local turbulence pattern is solely determined by the energy dissipation per unit mass, $\varepsilon$. The mean square velocity difference between two points of length $d_{max}$ is given by Batchelor [12] as follows:

$$\overline{v_c'^2} \approx (\varepsilon d_{max})^{2/3} \tag{35}$$

whereas $v_{r)max}$ is given by Levich [13] as:

$$v_{r)max} \approx [\varepsilon d_{max}(\rho_d/\rho_c)]^{2/3} (|\Delta\rho|/\rho_d)^{1/2} \tag{36}$$

where the subscript d identifies the dispersed phase.

When equations (35) and (36) are inserted into their respective places in equations (33) and (34), and the resulting equations are solved for $d_{max}$, the following equations can be obtained for the maximum particle size:

$$d_{max} = (\sigma We_{cr)2}/k_2\rho_c)^{3/5} \varepsilon^{-2/5} \tag{37}$$

and

$$d_{max} = (\sigma We_{cr)1}/k_1\rho_c)^{3/5}\varepsilon^{-2/5}(\rho_c/\rho_d)^{2/5}(\Delta\rho/\rho_d)^{-3/5} \quad (38)$$

where $k_1$ and $k_2$ are proportionality coefficients. These numerical coefficients probably have no great significance. They are set forth here only in order to stress the absence of large numerical coefficients in these formulas. Both $k_1$ and $k_2$ are the same order of magnitude of one.

Equations (37) and (38) have been used in literature to determine the maximum stable particle size in liquid–liquid, liquid–gas and gas–liquid dispersions irrespective of their differences in terms of fluid properties. The differences can be explained by comparing the expressions for fluid velocity relative to the particle, $v_{r)max}$, with the change in velocity of turbulence eddies over a distance equal to the dimension $d_{max}$ of the particle $(\overline{v_c'^2})^{1/2}$.

A comparison of equations (35) and (36) shows, that, with $\rho_d \leqslant \rho_c$, $v_{r)max} \ll (\overline{v_c'^2})^{1/2}$. In these cases, large-scale eddies of continuous phase completely entrain the fluid particle together with portions of fluid adhering to it, and transfer both as a single unit. The entrainment of particles by turbulence eddies is complete. Therefore, the second Weber number criterion, $We_{cr)2}$, which is based on $\overline{v_c'^2}$, mechanistically describes the fragmentation of drops and bubbles in a turbulent liquid flow for $\rho_d \leqslant \rho_c$. However, the disintegration of a drop in a turbulent gas stream occurs in a somewhat different manner. In this case, the entrainment of particles by turbulence eddies cannot be complete. The smaller-scale fluid motions are unable to entrain the particle, and, in relation to them, the particle acts as a motionless solid body. The fluid participating in these small-scale motions flows over the surface of the particle. In this case, inertial effects used in derivation of equation (36) play an important role in the mechanism of the drop's motion. In the case of $\rho_d \gg \rho_c$, from equations (34) and (35), it is evident that:

$$v_{r)max}/\overline{v_c'^2} \simeq (\rho_d/\rho_c)^{1/3} \quad (39)$$

which indicates that $v_{r)max}^2 \gg \overline{v_c'^2}$. Therefore, the disruptive forces based on $v_{r)max}$ become much larger than the disruptive forces generated by changes in eddies. In view of this brief discussion, the first critical Weber number criterion, $We_{cr)1}$, describes the disintegration of drops in a turbulent gas stream.

Several fluid particle break-up mechanisms have been discussed and the applicability of each mechanism has been clarified. However, as it is evident from equations (37) and (38), the key parameter in determining local $d_{max}$ is the turbulent energy dissipation rate, $\varepsilon$. Local turbulence and dissipation models for two-phase flow have not been established. Therefore, it is a challenge to develop a model for local correlation. First a one-dimensional model will be developed, and it is expected that in the turbulent core region this model can be used as a local correlation, since the turbulent characteristics may be approximated as uniform. However, in the wall shear layer, both turbulence and viscous effects become important. In this region, shear induced turbulence should be investigated.

3.2.2. *Break-up frequency*: $g(\nu')$. Several phenomenological models have been developed to predict the break-up frequency in liquid–liquid dispersions [4, 11, 14–16]. These models are heavily influenced by flow conditions and can be classified according to the hydrodynamic flow regime as follows:

BREAK-UP FREQUENCY MODELS

Turbulent flow models — Laminar flow model [11]

- Molecular decomposition analogy model [11]
- Dispersion hydrodynamics break-up models [4, 14, 15]
- Critical velocity break-up frequency model [11]
- Drop oscillation break-up frequency model [14]

As indicated above, models should be chosen with regard to the flow conditions. As an example, for dispersions in turbulent flow, the kinetic energy transferred by the eddies plays a dominant role in the break-up process. The imbalance between the kinetic energy and the surface energy is used to define the break-up frequency. In laminar flow or transition regimes, the imbalance would be between the shear forces and the surface forces on the particle, and many expressions for the break-up frequency in such environments can be found in the literature. The following model for break-up frequency in turbulent flow based on dispersion hydrodynamics is given here as an example. This model which was proposed by Coulaloglou and Tavlarides [4] uses the eddy-drop collision frequency and energy dissipation. It is dependent on the physical properties, particle size, and energy dissipation rate per unit mass as shown below:

$$g(\nu') = c_1(\varepsilon^{1/3}/\nu'^{2/9})\exp[-c_2\sigma/\rho_d(\varepsilon^{2/3}\nu'^{5/9})] \quad (40)$$

where the constants $c_1$ and $c_2$ are adjustable, to be determined from experiments according to the flow environment. It is to be noted that this expression is very similar to the one that can be derived using the molecular decomposition model except, in the latter, the continuous phase density was used instead of the dispersed phase density. Recently, this model has been improved by Tsouris and Tavlarides [17].

In the above derivation, the break-up rate was taken to be a function of the dispersed phase density. However, in gas–liquid systems, break-up is primarily governed by the density of the continuous liquid phase. The lack of an independent measurement of the break-up rate, as well as the use of several adjustable constants appearing in equation (40), prevent a direct use of equation (40) in bubbly flow systems. For example, comparisons of experimental data, for bubble break-up frequency with equation (40), which was

originally derived for drop break-up frequency, resulted in poor agreement [18].

3.2.3. *Number of daughter particle production*: $n(v')$. This parameter determines the average number of daughter particles produced by break-up of a parent particle of volume $v'$. Various experimental data indicate that 2–7 particles are produced in each break-up of liquid–liquid dispersions [14].

In the area of the bubble break-up process, the break-up process was considered to occur by break-up of a bubble into two daughter bubbles in random size. However, recently Prince *et al.* [19] and others have noted that bubble break-up is often accompanied by the production of two primary bubbles and a number of smaller fragments. Incorporation of this effect instead of binary break-up is expected to significantly alter the number of smaller bubbles and the interfacial area concentration predicted by the transport equations.

3.2.4. *Daughter particle distribution*: $\beta(v, v')$. This parameter is introduced due to the possible random production of non-equal daughter particles upon break-up. The simplest representation of daughter droplets volume density is to assume that two equal volume daughter particles are produced upon break-up. In relativity, a large number of non-equal daughter particles are produced upon break-up in a random fashion. Coulaloglou [20] used a normal distribution function as follows:

$$\beta(v', v) = (1/\sqrt{2\pi}\,\delta)\exp\left[-(v-\bar{v})^2/2\delta^2\right]. \quad (41)$$

This relation is based on the variance $\delta^2$ which is chosen in such a manner that 99.6% of the particles density lies within the volume range $0$–$v'$. $v'$ is the volume of the breaking parent drop and $\bar{v}$ is the mean volume of the daughter droplets.

The distribution given by equation (41) is only one example of several distribution functions that are available. For example, Hsia and Tavlarides [21] used beta distribution which gives 100% probability within two acceptable limits whereas Tsouris and Tavlarides [17] used a bimodal distribution function. It is important to note that $\beta(v', v)$ can be expressed in terms of any other suitable distribution function.

### 3.3 *Coalescence parameters*

3.3.1. *Description of coalescence processes.* While the maximum particle size was used as a criterion for the break-up process (where the particle size is considered stable when its size is below the maximum value), the minimum particle size can be used as a criterion for the initiation of the coalescence process (which is enhanced by the presence of small particles). It is assumed that there is a minimum stable particle size below which a pair of particles will coalesce upon colliding, and the ultimate coalescence process can be described in three consecutive stages. First, particles collide, and, upon the collision of two particles, the surfaces of the colliding particles flatten against each other; trapping a thin film between them under the action of the continuous phase. This film then drains over a period of time from an initial thickness of $h$ to a critical thickness, $h_c$, under the action of the film hydrodynamics. The hydrodynamics of the film depend on whether the film surface is mobile or immobile, and the mobility, in turn, depends on whether the continuous phase is pure or a solution. Finally, once the film reaches its critical thickness, it ruptures due to film instability, resulting in coalescence.

From the first step, it is seen that the coalescence rate is intimately connected to the particle collision frequency. In order to determine whether a given collision will result in coalescence, it is necessary to determine the collision efficiency. Two fluid particles will coalesce, provided they remain in contact for a period of time sufficient for the film between them to thin to the critical value necessary for rupture.

Considering a bubbly two-phase flow, collision may occur due to a variety of mechanisms summarized below:

COLLISION PROCESSES

| Turbulent fluctuations | Size dependent rise velocity differences | Wake entrainment | Shear layer induced velocity differences |
|---|---|---|---|

From the above, it is clear that collisions may result from the random motion of bubbles due to turbulence. In addition, bubbles of different sizes will have different rise velocities relative to continuous liquid phase which may lead to collision. A flow field generated at the wake of large Taylor bubbles entrains small bubbles into the Taylor bubble, resulting in a collision of small bubbles with a large bubble. Finally, bubbles located in a region of relatively high liquid velocity may collide with bubbles in a slower section of the velocity field. The first mechanism is a random process which largely depends on the fluctuating bubble motion and the inter-bubble distance. However, the latter three mechanisms highly depend on the particle size distribution and internal flow structure.

The coalescence process described above indicates that a clear understanding of the coalescence process depends on accurate knowledge of the minimum particle size, collision frequency and coalescence efficiency. These parameters are briefly discussed below.

3.3.2. *Minimum fluid particle size.* As described in Section 3.1, it is assumed that there is a minimum stable particle size below which a pair of particles will coalesce upon colliding. The equation that describes the minimum diameter for the absence of coalescence (i.e. the diameter below which coalescence will occur) can be obtained in the same way as the break-up equation. The adhesion force acts to hold the colliding fluid particles together. The energy of adhesion of two particles of equal diameter is given by Shinnar and Church [23] and Shinnar [22] as:

$$AE = C_1 d \tag{42}$$

where $C_1$ is a parameter dependent upon the critical rupture thickness, $h_c$.

A coalescence criterion can be developed by determining the critical value of the kinetic energy, which is given by $C_2\rho_c(\varepsilon d)^{2/3}$, to the adhesion energy. That is,

$$\frac{KE}{AE} = C_2\rho_c(\varepsilon d_{min})^{2/3}/C_1 d_{min}$$

$$= C_2\rho_c\varepsilon^{2/3} d_{min}^{8/3}/C_1 = \text{constant} \tag{43}$$

or

$$d_{min} = C_3/\rho_c^{3/8}\varepsilon^{1/4}. \tag{44}$$

Thomas [24] developed a coalescence criterion by performing a force balance similar to that presented above. However, the adhesion force was replaced by the surface tension force acting at the time of rupture. Thomas predicted the coalescence to occur if the drop diameter is less than the minimum diameter defined by:

$$d_{min} \sim 2.4(\sigma^2 h_c^2/\mu_c\rho_c\varepsilon)^{1/4}. \tag{45}$$

Equations (44) and (45) have been employed extensively in correlations for the minimum and mean diameters of dispersed phase drops in mechanically-agitated liquid–liquid systems [16, 25–27]. The development of phenomenological models for minimum bubble size in gas–liquid dispersions, however, has received comparatively little attention, even though such dispersed systems are of significant interest to bubbly two-phase flow hydrodynamics and heat transfer.

3.3.3. *Collision frequency*: $h(v, v')$. Based on the type of flow as described in the section on coalescence parameters, a variety of definitions for the collision frequency between two particles of diameters $d$ and $d'$ in liquid–liquid dispersions were proposed [11]. The suggested expression for the velocity averaged collision frequency in a uniform shear flow can be expressed as:

$$h(d, d') = 1.366(d+d')^3(\partial v/\partial r) \tag{46}$$

where $(dv/dr)$ is the velocity gradient perpendicular to the direction of liquid particle motion.

For turbulent flow, the velocity gradient can be replaced by:

$$\partial v/\partial r \simeq (\varepsilon/v)^{1/2}. \tag{47}$$

Therefore, the collision frequency becomes:

$$h(d, d') = 1.366(d+d')^3(\varepsilon/v)^{1/2}. \tag{48}$$

It should be noted that the drop size relative to the turbulent eddy size will affect the collision frequency. When the drops are small compared to the turbulent eddies, the drop velocity will be significantly affected by the eddies. When the drop density is equal to the density of the continuous phase, the drop velocity will be very close to the velocity of the continuous phase flow field. Under these conditions, the collision frequency will be determined by local turbulent flow characteristics. In this case, the collision frequency is given by:

$$h(d, d') = 0.618(d+d')^3(\varepsilon/v)^{1/2}. \tag{49}$$

The only difference between equations (48) and (49) is the constant coefficient.

When the drops are large compared to the turbulent eddies, the drop will be exposed to the eddies' stresses from all directions. This results in a random drop motion. This randomness in drop motion led researchers to consider the analogy between the collision of drops and the collision of molecules, as in the kinetic theory of gases. Based on this analogy, Rietema [28] proposed the collision frequency in terms of the average turbulent velocity fluctuations.

In addition to the collision frequency's dependence on particle size, the density of both dispersed and continuous phases plays an important role in shaping the collision frequency. When the drop density is significantly different than the density of the continuous phase, the drops move with different velocities based on their sizes. Therefore, the relative velocity between drops will be the primary cause of collision. This is known as the acceleration mechanism or size dependent rise velocity difference mechanism for collisions. This mechanism plays an important role whenever there is a significant difference in dispersed and continuous phase densities as in the case of bubbly flow.

Many correlations can be found in the literature for small and large sizes with equal or non-equal phase distributions. Recently, Prince and Blanch [18] in their predictive model for the coalescence rate in gas–liquid dispersions considered the cumulative contribution of three collision mechanisms due to turbulence, buoyancy and laminar shear.

3.3.4. *Coalescence efficiency*: $\lambda(v, v')$. In order to determine what fraction of fluid particle collision leads to coalescence events, it is necessary to define a coalescence or collision efficiency. The coalescence efficiency $\lambda(v, v')$ may be defined as the fraction of collisions between fluid particles of volumes $v$ and $v'$ that result in coalescence. This efficiency will be a function of the average contact time between bubbles and the average time required for particles to coalesce (the average coalescence time). The average coalescence time is the time required for the continuous fluid film trapped between the two colliding particles to thin to a critical value so that rupture, and consequently coalescence, can occur.

An expression for the efficiency is given by Coulaloglou and Tavlarides [4]:

$$\lambda(d, d') = \exp[-t_{coa}(d, d')/t_{con}(d, d')] \tag{50}$$

where $t_{coa}(d, d')$ is the average coalescence time of particles of diameters $d$ and $d'$, while $t_{con}(d, d')$ is the contact time for the particles.

Different models have been used to determine the

coalescence efficiency in turbulent and laminar flow regimes for liquid–liquid dispersions. These models are based on the biomolecular gas reaction analogy, sufficiency of the time of contact, impact of colliding particles as well as combined approaches for collision efficiency [11]. An expression for the coalescence efficiency in gas–liquid dispersions was proposed by Prince and Blanch [18].

## 4. FORMULATION OF THE INTERFACIAL AREA TRANSPORT EQUATION

### 4.1. *General functional dependence of various source and sink terms*

As derived from the statistical distribution transport equation, the local interfacial area transport equation is given by equation (12). For simplicity, it is possible to combine two terms related to the break-up process. Thus the break-up source term is defined as:

$$\phi_{\text{dis}} \equiv \phi_1 + \phi_2 \geqslant 0 \tag{51}$$

whereas the coalescence sink term is defined by:

$$\phi_{\text{co}} \equiv -(\phi_3 + \phi_4) \geqslant 0. \tag{52}$$

Hence, the interfacial area transport equation becomes:

$$\frac{\partial a_i}{\partial t} + \nabla \cdot a_i \vec{v}_i = \phi_{\text{dis}} - \phi_{\text{co}} + \phi_{\text{ph}}. \tag{53}$$

The various local mechanisms affecting the break-up and coalescence terms have been discussed in Section 3. Here we study the general functional dependence of these two terms. The fluid particle disintegration occurs mainly due to the turbulent fluctuation and interfacial stability. Therefore, locally it should depend on the particle size, $r_d$, turbulent intensity, $\overline{v_c'^2}$, and local relative velocity, $v_r$. Hence:

$$\phi_{\text{dis}} = \phi_{\text{dis}}(\overline{v_c'^2}, r_d, We) \tag{54}$$

where the Weber number is given by

$$We \equiv \frac{2\rho_c r_d v_r^2}{\sigma} \tag{55}$$

which scales the interfacial instability.

The coalescence process depends on the random collisions and the systematic wake entrainment. The collision is a strong function of the inter-particle distance and the amplitude of the fluctuating particle velocity. The latter depends on the continuous phase turbulent fluctuations. The wake flow structure depends on the particle Reynolds number, $Re_d$, and the particle size. The coalescence probability after a collision depends on the particle sizes and fluctuating velocity components. Thus:

$$\phi_{\text{co}} = \phi_{\text{co}}(\alpha_d, r_d, \overline{v_c'^2}, Re_d). \tag{56}$$

The turbulence intensity in dispersed flow may be related to the continuous phase Reynolds number, $Re_c$, and a distance from a wall.

### 4.2. *One-dimensional formulation and relation to experimental measurements*

The simplest form of the interfacial area transport equation can be obtained by applying the cross-sectional area averaging and reducing it to a one-dimensional form. This form of the interfacial area transport equation may have the most useful and practical applications in the existing one-dimensional two-fluid model. It can replace the traditional flow regime maps and regime transition criteria. The changes in the two-phase flow structure are predicted mechanistically by introducing the interfacial area transport equation. The effects of the boundary conditions and flow development are efficiently modeled by this transport equation. Such a capability does not exist in the current state-of-the-art. Thus a successful development of the interfacial area transport equation can make a quantum improvement in the two-fluid model formulation.

By applying the cross-sectional area averaging, the one-dimensional area transport equation becomes:

$$\frac{\partial \langle a_i \rangle}{\partial t} + \frac{\partial}{\partial z}\langle a_i \rangle \bar{v}_{iz} = \langle \phi_{\text{dis}} \rangle + \langle \phi_{\text{co}} \rangle + \langle \phi_{\text{ph}} \rangle + \langle \phi_w \rangle \tag{57}$$

where $\langle a_i \rangle$ denotes the area averaged interfacial area concentration. The term $\langle \phi_w \rangle$ stands for the wall nucleation source which can be important in boiling and condensation processes. The constitutive relation for this wall source term is discussed in Section 4.3. The average interfacial velocity is defined by

$$\bar{v}_{iz} \equiv \frac{\langle a_i v_{iz} \rangle}{\langle a_i \rangle}. \tag{58}$$

By using the local interfacial area measurement methods proposed by the authors [29–32], the following parameters can be measured simultaneously:

$$a_i = a_i(r, z) \tag{59}$$

and

$$v_{iz} = v_{iz}(r, z). \tag{60}$$

Under the adiabatic and steady conditions, there are no effects of phase changes; thus:

$$\frac{d}{dz}\langle a_i v_{iz} \rangle = \langle \phi_{\text{dis}} \rangle - \langle \phi_{\text{co}} \rangle \tag{61}$$

which shows the way to measure the right-hand side source and sink terms. First, two limiting cases are studied to isolate the break-up source term and the coalescence sink term. It is considered that there is a critical Reynolds number, $Re_c^*$, for a break-up process. Below this value, the break-up of fluid particles becomes insignificant. Hence, for $Re_e \ll Re_c^*$:

$$\frac{\mathrm{d}}{\mathrm{d}z}\langle a_i v_{iz}\rangle \simeq -\langle \phi_{co}\rangle. \tag{62}$$

Typically, this happens in low velocity bubbly flow. The gradual coalescence leads to the formation of Taylor cap bubbles. This is followed by the wake entrainment and development into slug flow. Hence, by measuring the left-hand side terms at two different axial locations, one obtains:

$$\langle \phi_{co}\rangle = -\frac{1}{\Delta z}[\langle a_i v_{iz}\rangle_2 - \langle a_i v_{iz}\rangle_1]. \tag{63}$$

These data represent the global changes in the interfacial area concentration.

For bubbly to slug flow transition, both the random coalescence and wake entrainment by Taylor bubbles can be significant. In order to measure the process of the wake entrainment, it is necessary to measure the characteristics of the large Taylor bubbles and small wake bubbles separately. The rate of coalescence due to the wake entrainment can be obtained from the separate measurements of interfacial velocities, interfacial area and void fractions of these two groups of bubbles using multi-sensor probe techniques [29].

From a geometrical consideration, the interfacial area concentration of a slug or churn-turbulent flow [33] is given by:

$$a_i = \frac{4.5}{D}\frac{\langle\alpha\rangle - \alpha_{gs}}{1-\alpha_{gs}} + \frac{3\alpha_{gs}}{r_{Sm}}\frac{1-\langle\alpha\rangle}{1-\alpha_{gs}} \tag{64}$$

where $\langle\alpha\rangle$, $\alpha_{gs}$, $D$ and $r_{Sm}$ are the average overall void fraction, average void fraction in the liquid slug section, hydraulic diameter and the Sauter mean radius of the small bubbles in the liquid slug section, respectively. The multi-sensor probes give all the parameters in the above equation. The first and second terms on the right-hand side give the separate contributions from the large Taylor bubbles and small bubbles in liquid slug. Thus, the total coalescence effect on the interfacial area can be measured. Furthermore, by measuring the velocity of Taylor bubbles, $v_{igs}$, and that of small bubbles, $v_{ib}$, by the multi-sensor probes, the influx of the small bubbles into the large slug bubble can be directly measured. This will give the sink term due to the entrainment alone.

For a break-up dominated section at high Reynolds number, $Re_c > Re_c^*$, the coalescence process may be neglected when the particle sizes are relatively large. Then:

$$\frac{\mathrm{d}}{\mathrm{d}z}\langle \alpha_i v_{iz}\rangle \simeq \langle \phi_{is}\rangle \tag{65}$$

or

$$\langle \phi_{dis}\rangle = \frac{1}{\Delta z}[\langle a_i v_{iz}\rangle_2 - \langle a_i v_{iz}\rangle_1]. \tag{66}$$

The boundary conditions for $\langle a_i\rangle$ can be changed by using different bubble injectors. For this group of experiments, relatively large bubbles which are unstable are injected at the inlet.

One extreme limit of this type of experiment has been already performed [34]. The detailed observation on the break-up process such as the wave growth of breaking bubbles are measured.

When two-phase flow is fully established, the break-up process and coalescence process should reach an equilibrium, thus:

$$\langle \phi_{dis}\rangle - \langle \alpha_{co}\rangle = 0 \tag{67}$$

which is a good check of the constitutive relations for break-up and coalescence processes.

The above three types of experimental data—(1) coalescence sink term data; (2) break-up source term data; and (3) fully developed equilibrium data—will be analyzed based on the general functional dependence of the constitutive relations for $\langle \phi_{dis}\rangle$ and $\langle \phi_{co}\rangle$. These phenomenological models should form the basis for the more mechanistic models discussed in Sections 2 and 3.

### 4.3. *Wall nucleation source term* $\langle \phi_w \rangle$

For boiling flow, the wall nucleation source $\langle \phi_w\rangle$ is the most important term. In view of this, an effort has been made to develop a reliable constitutive relation for $\langle \phi_w\rangle$ [1, 33]. It can be expressed by the following form:

$$\langle \phi_w\rangle = \frac{\xi_h}{A} Na f_{dp} \pi d_{dp}^2. \tag{68}$$

Here $\xi_h$, $A$, $Na$, $f_{dp}$ and $d_{dp}$ are the heated perimeter, flow area, nucleation site density, bubble departure frequency and bubble departure diameter, respectively. For a boiling system, the nucleation site density is given approximately by Kocamustafaogullari and Ishii [1] as follows:

$$Na = \frac{1}{d_{dp}^2}\left[\frac{2\sigma T_{sat}}{(T_w - T_{sat})\rho_g \Delta i_{fg}}\right]^{-4.4} f(\rho^*) \tag{69}$$

where $f(\rho^*)$ is a known function of a density ratio. The bubble departure diameter is given by:

$$d_{dp}^2 = 2.64\times 10^{-5}\theta\left(\frac{\sigma}{\Delta\rho g}\right)^{0.5}\left(\frac{\Delta\rho}{\rho_g}\right)^{0.9}. \tag{70}$$

Here, $\theta$ is the contact angle. The bubble departure frequency is expressed by:

$$f_d = \frac{1.18}{d_{dp}}\left[\frac{\sigma g \Delta\rho}{\rho_f^2}\right]^{0.25}. \tag{71}$$

Combining the above expressions, the nucleation site density can be calculated.

## 5. SUMMARY AND CONCLUSIONS

The interfacial area transport equation has been derived from the statistical model of the fluid particle

number transport equations. The basic mechanisms affecting the source and sink terms in the interfacial transport equation have been discussed in detail. The underlying physics and modeling approach to develop the closure relations for these terms are presented. The hydrodynamic effect can be divided into the break-up and coalescence of fluid particles. There are a number of different potential mechanisms which can lead to the break-up of fluid particles. For example, the local turbulence, high shear flow and interfacial instability can lead to substantial particle break-up. The coalescence process is caused by fluid particle collisions and subsequent break-up of the particle interface. The collision can be produced by turbulent fluctuations, size dependent rise velocity, wake entrainment and shear layer induced velocity difference. These phenomena affecting the break-up and coalescence of fluid particles are reviewed and a preliminary modeling approach is indicated.

The development of the one-dimensional interfacial area transport equation and the necessary experimental data to support the modeling effort are discussed. The changes in the flow regime can be predicted mechanistically by the interfacial area transport equation. The effects of the initial and boundary conditions on the flow structure development are effectively modeled by the present approach. Such capability does not exist in the present state-of-the-art. This novel approach should lead to a substantial improvement in the two-fluid model formulation.

*Acknowledgements*—This research is supported by the U.S. Department of Energy under the Office of the Basic Energy Sciences as a joint research program between Purdue University and the University of Wisconsin–Milwaukee. The authors would like to express their sincere appreciation to Dr O. P. Manley of DOE/BES for his support of this program and encouragement.

## REFERENCES

1. G. Kocamustafaogullari and M. Ishii, Interfacial area and nucleation site density in boiling systems, *Int. J. Heat Mass Transfer* **26,** 1377–1389 (1983).
2. G. Kocamustafaogullari, M. Ishii and I. Y. Chen, Correlation for nucleation site density and its effect on interfacial area, Argonne National Laboratory Report, ANL-82-32 (1982).
3. H. M. Hulburt and S. Katz, Some problems in particle technology, a statistical mechanical formulation, *Chem. Engng Sci.* **19,** 555–574 (1966).
4. C. A. Coulaloglou and L. L. Tavlarides, Description of interaction processes in agitated liquid–liquid dispersions, *Chem. Engng Sci.* **32,** 1289–1297 (1977).
5. A. D. Randolph and M. A. Larson, *Theory of Particulate Processes* (2nd Edn), p. 50. Academic Press, New York (1988).
6. D. Ramkrishna, The status of population balances, *Rev. Chem. Engng* **3,** 49–95 (1985).
7. J. N. Reyes, Statistically derived conservation equations for fluid particle flows. *Proceedings of ANS-THD*, Vol. 5, pp. 12–19, ANS Winter Annual Meeting, San Francisco (1989).
8. G. E. Taylor, The formation of emulsion in definable field of flow. *Proceedings of the Royal Society (London) Series*, Vol. A146, pp. 501–523 (1934).
9. S. Tomotika, Breaking up of a drop of viscous liquid immersed in another viscous fluid which is extending at a uniform rate. *Proceedings of the Royal Society (London) Series*, Vol. A153, pp. 302–318 (1936).
10. R. Kumar and N. R. Kulsor, The formation of bubbles and drops, *Adv. Chem. Engng* **8,** 255–368 (1970).
11. L. L. Tavlarides and M. Stamatoudis, The analysis of interphase reactions and mass transfer in liquid–liquid dispersions, *Adv. Chem. Engng* **11,** 199–273 (1981).
12. G. K. Batchelor, Pressure fluctuations in isotropic turbulence. *Proceedings of the Cambridge Phil. Society*, Vol. 47, pp. 359–371 (1951).
13. V. G. Levich, *Physicochemical Hydrodynamics*. Prentice-Hall, Englewood Cliffs, NJ (1962).
14. E. G. Chatzi and I. M. Lee, Analysis of interactions for liquid–liquid dispersion in agitated vessels, *Ind. Chem. Engng Res.* **26**(11), 2263–2267 (1987).
15. E. G. Chatzi, A. D. Garrielides and C. Kiparissides, General model for prediction of the steady-state drop size distribution in batch stirred vessels, *Ind. Engng Chem. Res.* **28,** 1704–1711 (1989).
16. S. G. Hatzikiriakos, R. P. Gaikwad, P. R. Nelson and J. M. Shaw, Hydrodynamics of gas-agitated liquid–liquid dispersions, *A.I.Ch.E. Jl* **36,** 677–684 (1990).
17. C. Tsouris and L. L. Tavlarides, On the breakage and coalescence models in turbulent dispersion, *A.I.Ch.E. Jl* (in press).
18. M. J. Prince and H. W. Blanch, Bubble coalescence and break-up in air-sparged bubble column, *A.I.Ch.E. Jl* **36**(10), 1485–1499 (1990).
19. M. J. Prince, S. Walters and H. W. Blanch, Bubble break-up in air-sparged biochemical reactors. In *First Generation of Bioprocess Engineering* (Edited by T. K. Ghose), p. 160 (1989).
20. C. A. Coulaloglou, Dispersed phse interactions in an agitated vessel, Ph.D. Thesis, Illinois Institute of Technology, Chicago, IL (1975).
21. M. A. Hsia and L. L. Tavlarides, Simulation and analysis of drop breakage, coalescence and micromixing in liquid–liquid stirred tanks, *Chem. Engng J.* **26,** 189–199 (1983).
22. R. Shinnar and J. M. Church, Predicting particle size in agitated dispersions, *Ind. Engng Chem.* **52,** 253–262 (1960).
23. R. Shinnar, On the behavior of liquid dispersions in mixing vessels, *J. Fluid Mech.* **10,** 259–275 (1961).
24. R. M. Thomas, Bubble coalescence in turbulent flows, *Ind. J. Multiphase Flow* **7,** 709–717 (1981).
25. M. F. Nishikawa, F. Mori and S. Fujieda, Average drop size in liquid–liquid phase mixing vessel, *J. Chem. Engng Japan* **28,** 12–19 (1987).
26. C. A. Coulaloglou and L. L. Tavlarides, Drop size distributions and coalescence frequencies of liquid–liquid dispersion in flow vessels, *A.I.Ch.E. Jl* **22,** 289–296 (1976).
27. M. Stamatoudis and L. L. Tavlarides, Effect of continuous phase viscosity on the drop sizes of liquid–liquid dispersions in agitated vessels, *Int. Engng Chem. Process Des. Dev.* **24,** 1175–1184 (1985).
28. K. Rietema, Segregation in liquid–liquid dispersions and its effect on chemical reactions, *Adv. Chem. Engng* **5,** 237–302 (1964).
29. M. Ishii, S. T. Revankar and W. H. Leung, Multi-sensor probe method for local measurement of two-phase flow characteristics. *Proceedings of the Japan–U.S. Seminar on Two-Phase Flow Dynamics*, pp. 443–460, Berkeley, CA (5–11 July 1992).
30. S. T. Revankar and M. Ishii, Local interfacial area measurement in bubbly flow, *Int. J. Heat Mass Transfer* **35,** 913–925 (1992).
31. G. Kocamustafaogullari, Z. Wang and W. D. Huang,

An experimental study on local interfacial parameters in a horizontal bubbly two-phase flow, *Int. J. Multiphase Flow* **17,** 553–572 (1991).
32. G. Kocamustafaogullari and W. D. Huang, An experimental description of spatial gas distribution in developing bubbly two-phase flow in horizontal channels. *Proceedings of ANS-THD*, Vol. 7, pp. 22–30, Atlanta, GA (1993).
33. J. Riznic and M. Ishii, Bubble number density and vapor generation in flashing flow, *Int. J. Heat Mass Transfer* **32,** 1821–1833 (1989).
34. J. W. Miller, An experimental analysis of large cap bubbles rising in an extended liquid, M.S. Thesis, Purdue University, West Lafayette, IN (1993).